TITLE:

Fundamental Study on Instability of Tunnel in Consideration of Post-Peak Strain Softening Behavior of Rock

AUTHOR(S):

AKAI, Koichi; HORI, Masayuki

CITATION:

AKAI, Koichi ...[et al]. Fundamental Study on Instability of Tunnel in Consideration of Post-Peak Strain Softening Behavior of Rock. Memoirs of the Faculty of Engineering, Kyoto University 1978, 40(2): 78-99

ISSUE DATE:

1978-06

URL:

http://hdl.handle.net/2433/281068

RIGHT:

京都大学学術情報リポジトリ
KURENAI 紅
Kyoto University Research Information Repository

Fundamental Study on Instability of Tunnel in Consideration of Post-Peak Strain Softening Behavior of Rock

By

Koichi AKAI* and Masayuki HORI**

(Received December 27, 1977)

Abstract

The main concerns of the present study are, firstly, to formulate the finite element analysis based on the principle of the "stress transfer method", by which the influnce of the post-peak strain softening behavior of rock, which is one of the intrinsic natures of rock like material, can be appropriately investigated with regard to instability of an underground cavity excavated in rock. Since very little information is available in rock mechanics literature on the post-peak strain softening behavior, and since no versatile constitutive law is as yet established to be readily employed in a numerical analysis, the analysis is presently conducted by assuming the idealized stress-strain relation and the modified Mohr-Coulomb failure criterion for practical usage. Secondly, the instability of a tunnel possibly caused by the excavation is studied. The analysis reveals a new finding with regard to the mechanism of the instability of a tunnel, such as the falling-off of the tunnel roof and rock burst, which has not been completely manifested so far. As would be anticipated, the shear failure might possibly be developed in a region where the stress concentration arises in relation to the initial stress system in the rock mass and the failure strength of rock. When the strain softening behavior is taken into consideration, the "most critical failure", (by which the rock loses completely the resitance due to the simultaneous emergence of the mode of shear failure as well as tensile failure), may be subsequently caused as a result of the stress release and the transfer from the previously failed element, the failure zone of which is formed as a cone in shape. This analytical solution is reasonably consistent with the field observation of the instability of a tunnel which takes place under a special stress condition, for instance, a region where a very high horizontal stress remains in the rock formations, as in Ontario, Canada. This is also true in a case where a tunnel is excavated in mountains where a very high overburden pressure might be acting.

1. Introduction

Because of the continuously rapid economic growth, the demand has been

* Department of Transportation Engineering

** Electric Power Development Co., Ltd.

increasing for large scale and proof civil structures, such as tunnels beneath the sea, underground and nuclear power generating stations. These developments invariably involve construction of underground cavities in rock. There exist in rock, however, numerous unkown factors which significantly govern the deformation and failure process of rock surrounding an excavation, *i.e.*, geological discontinuities with various orientation, in-situ stresses and the intricate natures of rock material. For a rational design of underground structure and safety of the construction performance, these factors must be precisely inquired into at the site of construction. Also, adequate laboratory tests should be undertaken to manifest the deformation and failure characteristics of rock. In addition to these investigations, considerations on logical constitutive models of rock material are necessary, capable of being conveniently applied to a design analysis with the use of numerical tools such as the finite element method.

To date, a failure strength at peak has been exclusively focused on, but a deformation process in a transient region from the peak to the residual state has not yet been significantly considered with regard to designing a structure constructed in rock and in analysing the deformation and failure of the surrounding rock. To achieve a simulation of the deformation and failure process of a rock mass as close as possible to a real situation, it is both significant and timely that an investigation on the failure behavior of the fractured rock be undertaken as well as on the pre-failure behavior of intact rock. The most effective way to study this problem is simply to determine the complete stress-strain characteristics of rock over a range of pre- and post-peak portions.

Next, another question arises as to how the complete stress-strain characteristics with inclusion of the strain softening behavior in the post-peak portion can be appropriately introduced into a numerical analysis. For a material which behaves as elasto-plastic and/or strain hardening, various investigations have been experimentally performed and several applicable constitutive laws have been logically deduced. These constitutive laws have successfully been introduced into the finite element analysis[1]. Nevertheless, since investigations on fractured rock which exhibits post-peak strain softening have seldom been conducted both experimentally and mathematically, no constitutive law that can be readily employed for a numerical analysis is available at this time. There still remain some difficulties as regards a mathematical and numerical treatment to be settled before establishing a versatile constitutive law for such material as this.

As a fundamental and numerical approach for the consideration of the post-peak strain softening behavior of material into the stress and deformation analysis, it is briefly described in this study how the stress transfer method is successfully

employed in the finite element analysis, by postulating an idealized stress-strain relation. The main concern of this study is to investigate the influences of the post-peak strain softening on the stability of a circular opening, such as a tunnel excavated in rock, in its circumferential area. The analysis is similarly conducted for an elastic, perfectly plastic material and the results are compared with those obtained for the strain softening material.

2. Stress-Strain Curve for Strain Softening Material

Most rock materials exhibit a non-linear behavior with some degree of pre-peak portion, being caused by crack closure, cracking of the individual grains and/or a loosening of the grain boundaries. Brace has categorized the stress-strain curve of rock material into four regions as regards behavior[2]. In addition to this non-linearity rock material exhibits more or less "strain softening" or "work softening", *i.e.*, a decrease of strength during further shear-straining after a peak strength has been reached (see Fig. 1 (a)). In the final stage, a large deformation will take place associated with a mobilization of the shear resistance of the rock material, at which a residual strength is attained. Accompanied with a complete stress-strain curve, the knowledge of the deformation and strength behavior of rock is essential for determining the ultimate stability of underground excavations in rock. However, studies on the strain softening behavior of rock material have seldom been conducted both experimentally and mathematically. From the experimental aspect, the complete stress-strain curve is obtained only by using a stiff testing machine, but not by the conventional (soft) testing machine. The strain softening behavior of fractured rock* depends exclusively upon the relative stiffness of the specimen and the testing machine

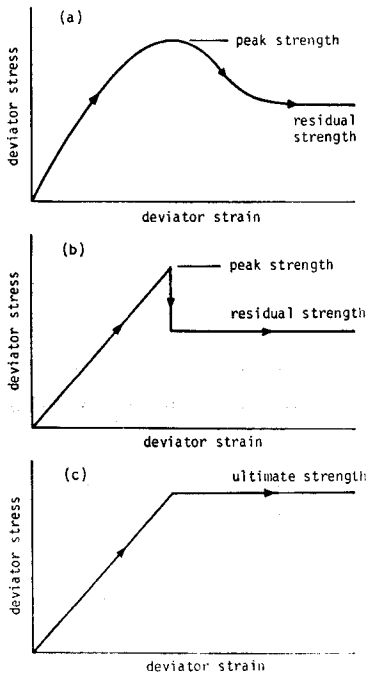

Fig. 1. Stress-strain curve of rock material: (a) actual, (b) idealized strain softening and (c) elasto-plastic curve.

* According to Bieniawski, *et al.*[3], the definition of fracture is "the failure process by which new surfaces in the form of cracks are formed in a material or existing crack surfaces are extended. Various stages of fracture may be visualized, namely, fracture initiation fracture propagation (stable and unstable) and strength failure".

system[3]. Most generally, when a tested rock specimen is sound intact rock, a higher stiffness of the testing machine is inevitably required, and *vice versa*. Very little information is available in literature about the mathematical formulation of the constitutive law, taking into account the strain softening behavior. This is mainly due to the difficulty of interpreting the intrinsic mechanism of a failure process through use of a concept of the classical theory of plasticity. For instance, the strain softening flow law violates Drucker's postulate[4].

Nevertheless, it has been manifested throughout the successive experiments carried out by Bieniawski that there emerge several important factors which govern the nature of the strain softening behavior of rock material[5),6]. A summarization of the results obtained follows. An increasing confining pressure tends to flatten the negative slope of the stress-strain curve which emerges in the post-peak portion. This fact indicates that as the confining pressure increases, the rock material predominantly possesses a characteristic of ductile behavior rather than brittle behavior. A steeper negative slope will also generally be obtained for rock materials having a higher compressive strength or a higher modulus of elasticity than for materials having a lower value of strength or modulus.

The post-peak strain softening behavior is highly affected by a strain rate as well, associated with the creep characteristics of the rock material. Namely, as the strain rate decreases, the negative slope tends to be flat, and, a ratio of the positive slope in the pre-peak portion to the negative slope monotonously increases[6]. Furthermore, Bieniawski conducted a test in which he first carried out compression tests on rock specimen with the application of two different constant strain rates, *i.e.*, the higher and the lower rates, and obtained two complete stress-strain curves for each specimen. Secondly, another set of specimens is provided, compressing up to a certain stage in the post-peak portion with either of the strain rates employed in the test previously conducted. Then, the specimen is further compressed by immediately changing the strain rate to another, respectively, *i.e.*, from the higher to the lower strain rate and *vice versa*. Consequently, the stress-strain curve obtained after the change of the strain rate tends to gradually follow the original curve which is obtained for the constant strain rate correspondingly. This experimental fact may then draw the conclusion that the residual strength of rock material is clearly a function of the strain rate with which the material is compressed.

As stated above, various factors which govern the post-peak strain softening behavior have gradually been clarified so far with numerous well controlled tests on fractured rocks. Nevertheless, there still remain unknown natures of strain softening behavior to be solved, for example, dilatancy characteristics and time depende-

ncy[7]. To establish an adequate constitutive law of the strain softening as well as the strain hardening behavior of rock material which allows the implying of the mechanical nature of rock material, and is ready to use for numerical applications, a great deal of experimental research may further be required.

In connection with a finite element approach described later on, the stress-strain curve indicating the post-peak strain softening behavior of rock material might be possibly idealized, as shown in Fig. 1 (b), for the main concern of the present study to investigate the influences of strain softening behavior on the stability problem of rock. The curve shows that the material behaves linearly elastic in the pre-peak portion, and that the stress drops abruptly from the peak to residual strength level. It should be noted that this replacement of the actual stress-strain curve to the idealized curve would be rather conservative for determining the ultimate stability of rock, with regard to excavation and other rock mechanics problems. A similar idealization has been reasonably made for conventional elasto-plastic material (see Fig. 1 (c)). An analysis will be conducted both for the strain softening and elasto-plastic materials, and the results will be compared with each other.

3. Failure Criterion Employed in the Analysis

The Mohr-Coulomb failure criterion has been adequately advocated to determine

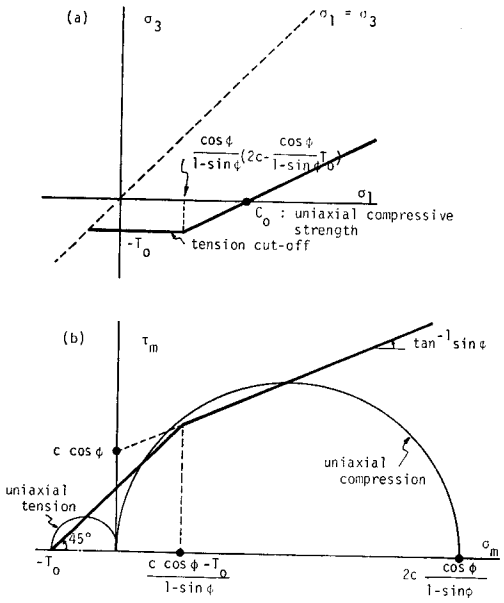

Fig. 2. The modified Mohr-Coulomb failure criterion: (a) σ_1-σ_3 plane and (b) τ_m-σ_m plane.

the failure strength of materials such as rocks, because of the simplicity and reasonably adequate interpretation of experimental results. Especially, it is usefully employed in analysis for a practical usage. In the present study, the Mohr-Coulomb theory is therefore properly chosen to describe both the peak and the residual strength of strain softening material with some modification.

Paul has pointed out that despite the propriety of the Mohr-Coulomb theory for the shear failure of brittle materials, it can not satisfactorily explain several features of other laboratory tests such as simple tension test and simple torsion test[8]. To remove this deficiency, he introduced a suitably chosen "tension cut-off" in the stress diagram as shown in Fig. 2 (a). The modified criterion is therefore given, as a locus of the maximum shear stress and the mean stress[9], by

$$\tau_m=\sigma_m \sin\phi+c\cos\phi \qquad \sigma_m>\frac{c\cos\phi-T_0}{1-\sin\phi} \qquad \cdots\cdots\cdots(1)$$

$$\tau_m=\sigma_m+T_0 \qquad \sigma_m\leq\frac{c\cos\phi-T_0}{1-\sin\phi} \qquad \cdots\cdots\cdots(2)$$

in which, c denotes the cohesion, ϕ the internal friction angle and T_0 the uniaxial tensile strength. τ_m and σ_m are the maximum shear stress and the mean stress, respectively, which are given by

$$\tau_m=\frac{\sigma_1-\sigma_3}{2}, \qquad \sigma_m=\frac{\sigma_1+\sigma_3}{2} \qquad \cdots\cdots\cdots(3)$$

in terms of the maximum and minimum principal stresses. Fig. 2 (b) shows the modified Mohr-Coulomb criterion given by Eps. (1) and (2) on the $\tau_m-\sigma_m$ plane, in which Mohr's stress circles are also depicted for uniaxial compression and uniaxial tension. It is evident from a simple operation that the uniaxial compressive strength C_0 can be expressed by

$$C_0=2c\frac{\cos\phi}{1-\sin\phi} \qquad \cdots\cdots\cdots(4)$$

Fig. 3 diagrammatically indicates a classification of the type of failure in relation to the state of the principal stresses currently occurring at failure. Region A is for tensile failure, whereby this case can possibly emerge in either state of stress of $0>\sigma_1>\sigma_3$ or $\sigma_1>0>\sigma_3$. In regions B and C, shear failure is brought about. The former case will be incurred by such a stress condition where the maximum principal stress is positive and the minimum principal stress is negative, being accordingly referred to as a combined failure. The latter will be a resultant of the compressive stresses of σ_1 and σ_3, preferably called just shear failure.

Prescribing the ultimate failure strength by the modified Mohr-Coulomb crite-

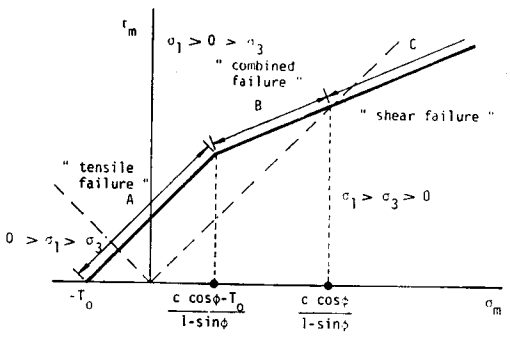

Fig. 3. Classification of failure mode.

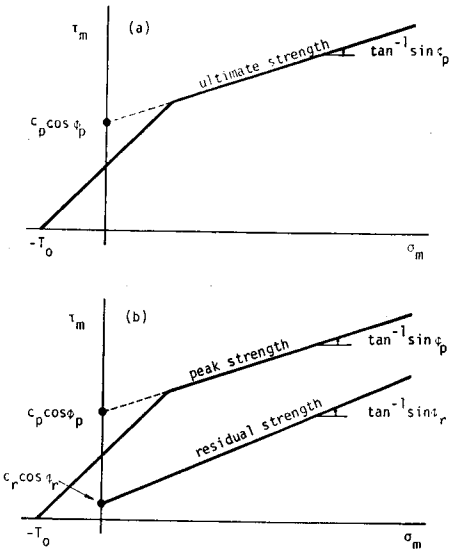

Fig. 4. The modified Mohr-Coulomb criterion employed in the analysis for (a) elasto-plastic material and (b) strain softening material.

rion, that analysis for the elasto-plastic material is conducted using the notations of the strength parameter as presented in Fig. 4 (a). On the other hand, for the strain softening material, the peak strength of the material is given by the modified Mohr-Coulomb criterion with the notations of the strength parameter as shown in Fig. 4 (b). In addition to the peak strength, an assumption might be most probably accepted that the residual strength would also be reasonably prescribed by the Mohr-Coulomb criterion as shown in Fig. 4 (b) where ϕ_r denotes the internal friction angle in the residual state and c_r the cohesion.

4. Finite Element Approach by Using Stress Transfer Method

Since the finite element method has been, in recent years, considerably refined, and moreover since the capacity of the computer has been tremendously extended, it becomes more versatile and can possibly deal with various types of nonlinear and non-homogeneous problems. The "iterative stress release and transfer" method (simply called stress transfer method) was first used by Zienkiewicz *et al.*[10] in connection with the stress analysis in the socalled "no tension" material. This method has been proved to be extremely simple in use and always convergent. The same approach, appropriately modified, will be presently employed to handle the perfectly plastic and the post-peak strain softening behaviors.

Lo and Lee[11] successfully employed the stress transfer method to solve the stress distribution in a slope of strain softening material with the idealized stress-strain curve being the same as shown in Fig. 1 (b). They referred to the mechanism of the progressive failure of the slope, being incorporated into the equilibrium method for the stability analysis. In their analytical scheme, a very small value of modulus was assigned to the failed element in the sense that a large deformation is induced, and as a result, the material flows in the residual state. Consequently, a new stiffness matrix must be generated in each subsequent iteration of stress release and transfer. Zienkiewicz *et al.*, however, pointed out that this scheme has been tried with success in some cases, but unfortunately its convergence can not be guaranteed and is always slow[10]. Kawamoto and Saito also used the stress transfer method to take the post-failure behavior into account by assuming the elasto-plastic behavior of material. They also reasonably allowed tensile failure of the material in the analysis[12]. The discussion was conducted for the stability of the circumferential area of the circular opening in an infinite plate subjected to external stress. The present analysis employed in this study is essentially the same as those described above, but the scheme is refined in some parts for practical orientation, and explained in some detail below.

The analysis will be carried out for two idealized materials, *i.e.*, the elasto-plastic and the strain softening material with the idealized stress-strain curve represented in Fig. 1. However, the analytical scheme of the finite element approach by using the stress transfer method is essentially the same for the two different materials. Therefore, a comprehensive explanation of the scheme employed is given solely for the material having the post-peak strain softening behavior on behalf of the two different materials. The scheme for the material having elastic and perfectly plastic behavior should be somewhat simpler in the treatment.

As represented in Fig. 1 (b), the curve is comprised of a linearly elastic pre-peak portion with the modulus E and the linear post-peak portion representing the residual state. Associated with the failure criterion described in the previous section, the following procedures may be adopted for a stress analysis.

(1) Computation of stresses and strains in each element is firstly made, assuming the material to be a linearly elastic body with the modulus E, by the conventional way of the finite element method.

(2) The computed maximum shear stress $(\sigma_1-\sigma_3)/2$ is then compared with the inherent peak strength of the material, which is uniquely prescribed by the failure criterion associated with current state of stresses. As is classified, there might possibly be an anticipated occurrence of three types of failure related to the state of stresses, namely, shear failure, combined failure and tensile failure. It would be,

however, appropriate to classify these three features of failure into just two groups, that is, shear failure and tensile faliure.

After the stresses and strains have been computed, it will be identified whether the minimum principal stress σ_3 in each element may or may not exceed the tensile strength T_0. No matter whether the maximum principal stress σ_1 is positive or negative, the element in which σ_3 is less than T_0 is then considered to have failed with tensile failure.

The numerical scheme is therefore briefly explained one by one for each feature of failure.

(i) Shear failure

At this failure, the state of stress is that σ_1 is positive and σ_3 is positive or negative, but is greater than $-T_0$. Mohr's stress circle, representing the state of stress which has been computed from the stage (1), is schematically shown in Fig. 5, indicating that the computed maximum shear stress exceeds the peak strength.

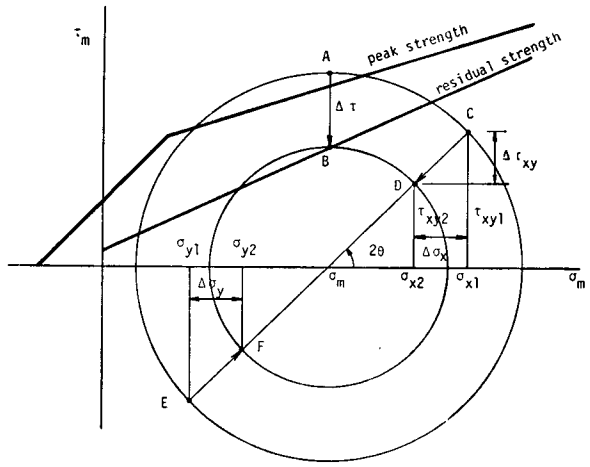

Fig. 5. Reduction of stress to the residual state in the overstressed element.

For each of these "overstressed" elements, the maximum shear stress is brought down from point A to the residual state at point B, by removing from the element an excess amount of the shear stress $\Delta\tau$ given by

$$\Delta\tau=\left(\frac{\sigma_1-\sigma_3}{2}\right)_{\text{at A}}-\left(\frac{\sigma_1-\sigma_3}{2}\right)_{\text{at B}} \qquad \cdots\cdots\cdots(5)$$

Maintaining the mean stress $(\sigma_1+\sigma_3)/2$ and the direction of the principal stress temporarily unchanged (see Fig. 5), the stress change $\{\Delta\sigma\}$ in the $x-y$ plane, corresponding to the resultant change of the maximum shear stress, is given by

$$\{\Delta\sigma\}=\begin{Bmatrix}\Delta\sigma_x\\ \Delta\sigma_y\\ \Delta\tau_{xy}\end{Bmatrix}=\begin{Bmatrix}-\Delta\tau\ \cos 2\theta\\ \Delta\tau\ \cos 2\theta\\ -\Delta\tau\ \sin 2\theta\end{Bmatrix} \qquad \cdots\cdots(6)$$

where θ is the inclination of σ_1 to σ_x. These components of overstress have to be eliminated, without permitting any point in the structure of the finite element to be displaced. In order to maintain equilibrium, however, restraining forces have to be applied to the structure, which are equal in magnitude but opposite in sign to those forces associated with the overstress. A new set of the restraining forces can therefore be generated, based on the principle of virtual work:

$$\{F\}=\int_v[B]^T\{-\Delta\sigma\}dv \qquad \cdots\cdots(7)$$

where

$\{F\}$ =set of restraining forces

$[B]^T$ =transpose of the position matrix

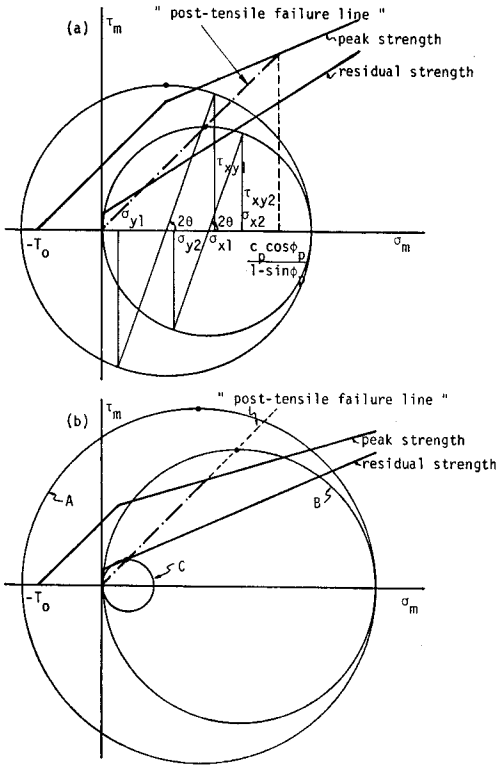

Fig. 6. (a) Stress transfer in the element failed with the mode of tensile failure and (b) the most critical failure with the shear failure as well as the tensile failure caused simultaneously.

$\{-\Delta\sigma\}$=stress increments equal and opposite to $\{\Delta\sigma\}$

$\int_v dv$ =volume of element.

(ii) Tensile failure

Kawamoto and Saito[12] have adequately postulated that once tensile failure has occurred, any tensile stress would not be sustained in this element any more. This postulate is reasonably accepted herein in the present study. A situation of tensile failure possibly occurred is represented in Fig. 6 by Mohr's stress circle.

Fig. 6 (a) expresses Mohr's stress circle in which the state of stress has been computed in stage (1), assuming the material to be linearly elastic. Since the computed tensile stress exceeds the tensile strength T_0, the element should consequently fail by the mode of tensile failure, and can not therefore sustain tensile stress any more. This leads to a subsequent situation where the state of stress in the element is transferred to a uniaxial state of stress as shown in the figure. The maximum shear stress in a new state of stress should therefore be on the "post-tensile failure line" which is given by

$$\tau_m=\sigma_m \qquad \cdots\cdots\cdots\cdots(8)$$

As before, it is assumed that the maximum principal stress σ_1 and the direction of the principal stress in the element are temporarily maintained unchanged. From the figure, the stress change to be eliminated is then given by

$$\{\Delta\sigma\}=\begin{Bmatrix}\Delta\sigma_x\\ \Delta\sigma_y\\ \Delta\tau_{xy}\end{Bmatrix}=\begin{Bmatrix}\sigma_{m2}(1+\cos 2\theta)-\sigma_{x1}\\ \sigma_{m2}(1-\cos 2\theta)-\sigma_{y1}\\ \sigma_{m2}\sin 2\theta-\tau_{xy1}\end{Bmatrix} \qquad \cdots\cdots\cdots\cdots(9)$$

where the mean stress σ_{m2} is given by $\sigma_1/2$. Further, a set of the restraining forces to be re-distributed to the structure is generated by Fq. (7), as is also the case for the shear failure.

Meanwhile, there can possibly occur a case, where for an element which has initially been identified to fail with tensile failure (circle A in Fig. 6 (b)), and where its state of stress has appropriately been transferred conforming to the scheme mentioned heretofore (circle B), the resultant maximum shear stress still exceeds the peak strength determined by a new state of stress. It would be supposed that such an element as this might have completely failed in a physical sense. Numerically, however, it will be treated as regarding the element to be in a corresponding residual state as represented by circle C. As before, a total of the stress change throughout such a transfer process can be therefore given by

$$\{\Delta\sigma\}=\begin{Bmatrix}\Delta\sigma_x\\ \Delta\sigma_y\\ \Delta\tau_{xy}\end{Bmatrix}=\begin{Bmatrix}\sigma_{m2}(1+\cos 2\theta)-\sigma_{x1}\\ \sigma_{m2}(1-\cos 2\theta)-\sigma_{y1}\\ \sigma_{m2}\sin 2\theta-\tau_{xy1}\end{Bmatrix} \qquad \cdots\cdots\cdots\cdots(10)$$

where σ_{m2} is the mean stress of Mohr's stress circle C and is given in terms of the residual strength parameters by

$$\sigma_{m2}=c_r\frac{\cos\phi_r}{1-\sin\phi_r} \qquad \cdots\cdots\cdots\cdots(11)$$

and σ_{x1}, σ_{y1} and τ_{xy1} are the components of stress expressed by the circle A. Therefore, supposing that the cohesion c_r of the residual strength is zero, this element would not be able to sustain any stress, and the stresses presently subjected to the element would have to be completely released. The calculation of the restraining forces then follows as before.

(3) This stage is to superpose the restraining forces for the elements which have failed either because of shear failure or tensile failure or both, and to re-analyse the structure for the effect of such forces. By this operation, the adjacent element surrounding the previously failed elements may possibly fail, and the failure zone may therefore expand gradually during the iterative process of stress release and transfer. Computation in this stage can be readily performed by regarding the structure as a linearly elastic body, namely, without changing the stiffness matrix.

The computed state of stress in each element is again identified by the failure criterion. The state of stress in the element which has failed because of shear failure in the previous stage, should be greatly reduced to the residual state, while it should be reduced to the uniaxial state of stress for the element which has previously been subjected to the tensile failure.

(4) Iteration of stages (2) and (3) will be continued until the state of stress in a failed element due to shear failure yields to the residual state prescribed by the failure criterion exactly or within an acceptable limit of error and/or similarly for an element which has failed because of tensile failure, it yields to the corresponding state of stress as described in detail at stage (2).

5. Application of the Method to Tunnel Problems

The ordinary and rudimentary program of the finite element method commonly used for elastic analysis (*e.g.* refer to 13) has been appropriately modified so that it can be properly employed for the elasto-plastic and/or the strain softening analysis on the basis of the stress transfer method briefly mentioned in the previous sections. The employed program is basically established for a triangle finite element in which stresses and strains are assumed to be constant and for a plane strain condition. However, when assessing the numerical distribution of the stress and strain in the structure, and when discussing the failed element in relation to the failure criterion, the stress and strain in the two adjacent triangle elements are properly

averaged so as to represent the values at the center point of these two elements. An analysis is tentatively conducted to manifest a possible instability in the circumferential area around a circular opening such as a tunnel excavated in rock.

(a) finite element mesh

The configuration and mesh used in the solutions are illustrated in Fig. 7 (a).

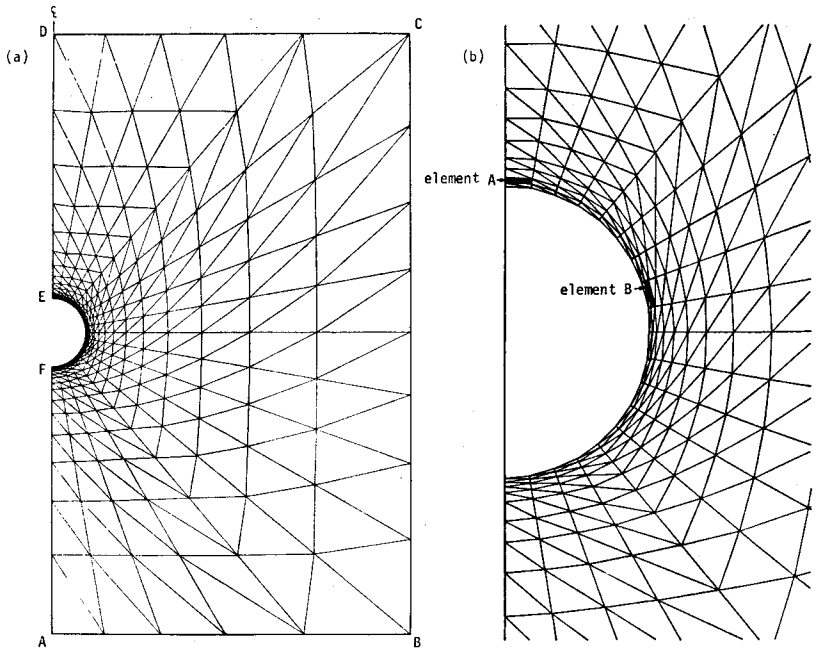

Fig. 7. Configuration and mesh used in the analysis: (a) whole boundary of the finite element mesh and (b) mesh around a circular opening.

Altogether, 532 triangle elements and 294 nodal points are employed. Since the stress concentration and the irregularity of the stress gradient are easily anticipated to happen in a circumferential area near the tunnel opening by the excavation, the mesh is therefore generated finely in this region, and coarsely in a region remote from the tunnel opening as gradual. Fig. 7 (b) is the mesh magnifying a portion around the tunnel. The condition of the prescribed displacement at the remote boundary of the mesh is given whereby the displacement is confined not to take place in the x-direction, and to be free in the y-direction along the lines B-C, D-E and F-A, and *vice versa* along A-B and C-D.

(b) initial stress and strength parameters employed

For a design purpose of the structure and safety of a construction performance in rock, it is necessary to know the in-situ stress system existing in the rock mass before excavation or construction. In recent years it has been noted that the in-

situ stress system actually existing differs in some degree from expectations, in general, associated with the geological history and tectonic activity of rock[14]. An accurate knowledge of the in-situ initial stress system is therefore a prerequisite for any design and construction performance, which can be done only by elaborately carrying out an appropriate and feasible stress measurement at place to place in the site of construction.

In the finite element analysis, the manner of the application of loads must be essentially related to the initial stress system. The excavated surface, on which the stress is removed and therefore free from stresses, can be analytically generated by applying on the expected surface a set of loads equal in magnitude and opposite in sign to those calculated from the initial stress system. For simplicity, and also as an extreme case of stress field generally encountered in actual rock mass, in the present study, a circular tunnel is excavated in an infinite rock mass which is subjected to a uniaxial stress, p, as schematically illustrated in Fig. 8 (a). As

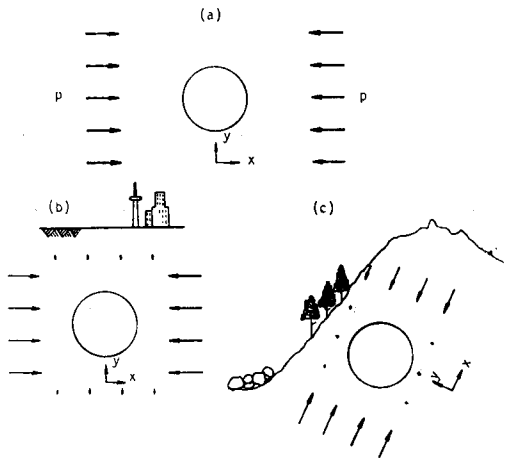

Fig. 8. (a) Circular opening excavated in the medium in the uniaxial stress field with the external stress p. (b) a tunnel excavated in rock with high horizontal stress and (c) a tunnel excavated in mountain.

such, this initial stress system before excavation may reasonbly simulate the situation where a shallow tunnel is excavated in rock subjected to a high horizontal stress remaining in rock formation, which is generally found in certain districts, such as Ontario, Canada[15] and North Europe[16]. In these areas, the horizontal stress is exceedingly higher than the overburden stress at a moderate depth relevant to engineering problems, as shown in Fig. 8 (b). The other similar situation may arise when a tunnel is excavated in a mountain as illustrated in Fig. 8 (c). As may be immagined, the overburden pressure might be significantly large, while the

lateral stress might be minute due to a lack of confinement.

The strength parameters employed in the analysis are as below, which are given in an expression of non-dimensional form normalized by the uniaxial stress p:

$$\frac{c_p}{p}=0.5 \qquad \frac{c_r}{p}=0 \qquad \frac{T_0}{p}=0.2$$

$$\phi_p=\phi_r=30^\circ$$

in which the notations used have been previously explained in Section 3. It is therefore evidently known according to Eq. (4) that the ratio of the uniaxial compressive strength of the material presumed for the remote stress p is given by

$$\frac{C_0}{p}=\frac{2c}{p}\frac{\cos\phi}{1-\sin\phi}\fallingdotseq 1.7$$

In addition to this ratio, it is of special interest to know the ratio of the uniaxial compressive strength to the tensile strength, computed as

$$\frac{C_0}{T_0}\fallingdotseq 8.7$$

These strength parameters employed may not be realistic, but they may possibly be underestimated. However, they are boldly used to exaggerate the possible instability brought about around a tunnel.

Meanwhile, the elastic constants used in the analysis are also given in the non-dimensional form as follows:

$$\frac{E}{p}=2000 \qquad \text{and} \qquad \nu=0.2$$

where E and ν denote Young's modulus and Poisson's ratio, respectively.

(c) results

Assuming the material to be linearly elastic, the computation has been performed prior to the subsequent step for the elasto-plastic and/or the strain softening analysis. Well known is the stress distribution around a cicular opening in an infinite, elastic medium in a uniaxial stress field. Fig. 9 represents the computed contours of the maximum and minimum principal stresses in a circumference of the opening, described with the ratio to the remote stress p. From these contours, the general trend of stress distribution in rock after excavation may be obviously acquired. The maximum stress concentration is incurred at the crown and invert, the magnitude of which is theoretically three times the remote stress. On the other hand, at the springline, the maximum tensile stress is induced tangentially to the surface with a magnitude equal to the remote stress. The tensile stress zone is generally formed as a butterfly shape in a symmetrical direction at about 45°, with

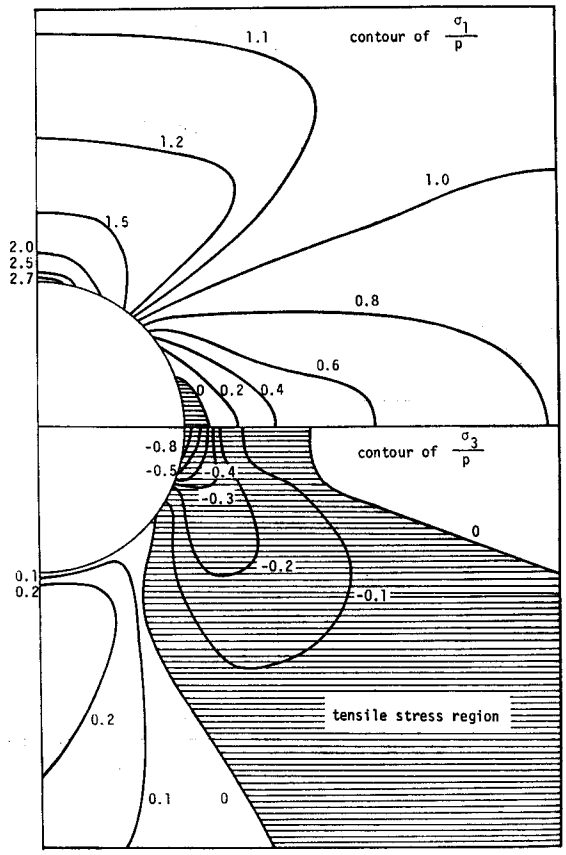

Fig. 9. Contours of the maximum and minimum principal stress induced around a circular opening by the excavation (linearly elastic analysis).

a horizontal axis, as indicated by the shaded area.

If one or more elements should be identified to be in a state of failure in accordance with the prescribed failure criterion, the iterative treatment of stress release and transfer is then begun. During the process of iteration, other adjacent elements to the originals may possibly fail because of an additional change of stress. The failure zone should, however, cease to expand after several cycles of iteration, and therefore the state of stress in the failed element gradually approaches the proper state. If the failure zone expands unduly without ceasing, it is then regarded that the whole structure will collapse. In the present case, both for the elasto-plastic and the strain softening analysis, a convergence has been obtained with less than 0.5% of error after ten iterations. As would be anticipated, a convergence for the elasto-plastic analysis may be achieved more rapidly to some extent than for the strain softening analysis, since a degree of stress release and transfer in the strain

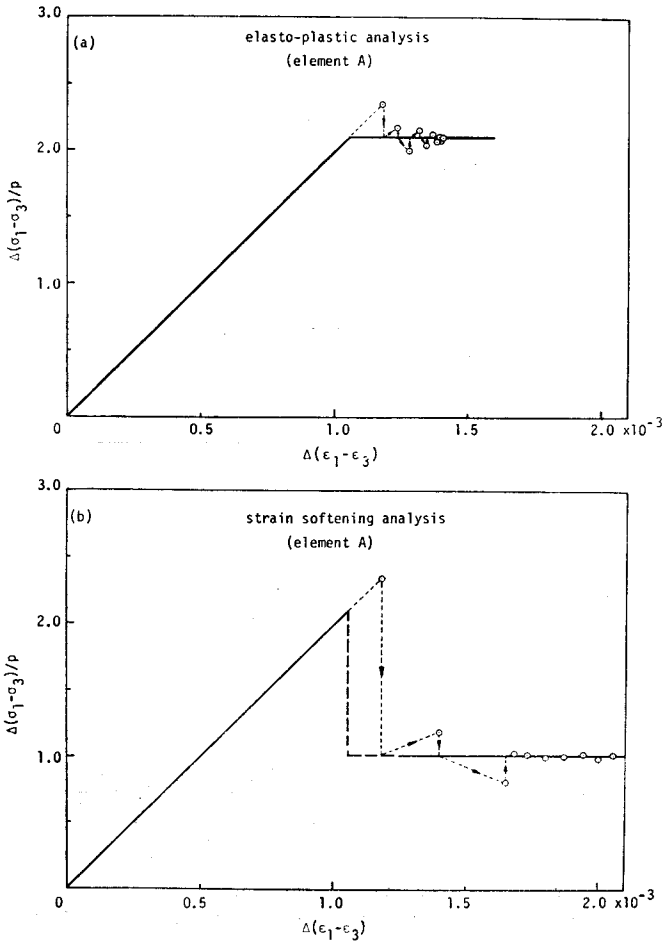

Fig. 10. Convergence of solution with iterative process of stress release and transfer: (a) the elasto-plastic analysis and (b) the strain softening analysis.

softemng analysis is virtually greater than in the elasto-plastic analysis. To illustrate the process of convergence, the current stress-strain relation at each iteration in the element A shown in Fig. 7 (b), which has failed with a mode of shear failure, is visually represented in Fig. 10 (a) and (b) for the elasto-plastic and the strain softening behaviors, respectively. It may be noted that a larger deformation takes place obviously in the post-peak portion of the strain softening behavior compared to the other. Meanwhile, once tensile failure has occurred in an element, the tensile stress existing is basically removed such that the state of stress in the element arrives finally at a proper uniaxial compressive state of stress. Fig. 11 shows the iteration process for the elimination of the tensile stress in element

B shown in Fig. 7 (b).

Development of a failure zone incurred in the circumference of a tunnel is of special interest in relation to the instability accompanied with the excavation of a tunnel. The final solution of the developed failure zone is illustrated in Fig. 12, separately for the two cases of the elasto-plastic and the strain softening analysis. It can be recognized, as presumably expected, that in the case of elasto-plastic

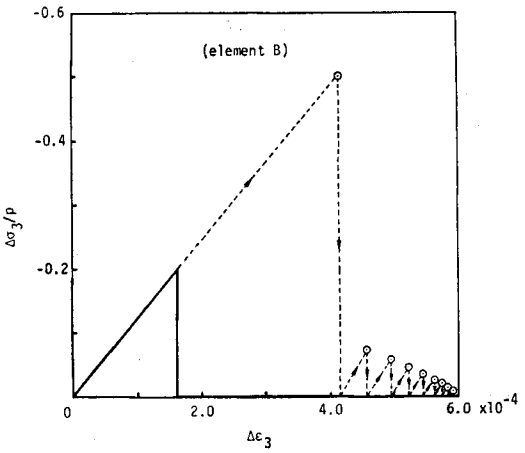

Fig. 11. Iterative process of elimination of tensile stress in the element failed with the mode of tensile failure.

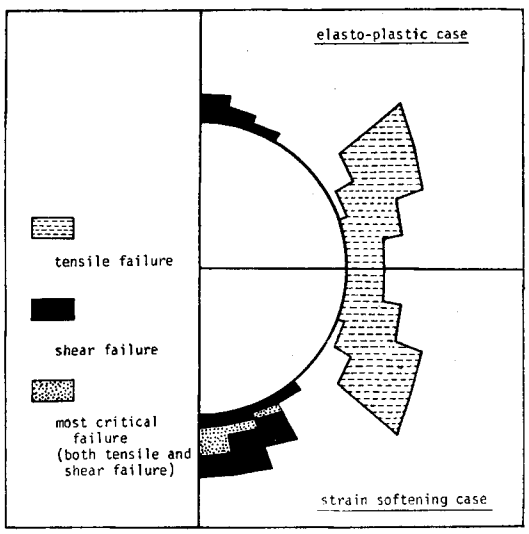

Fig. 12. Failure zone developed in the circumference of the tunnel: (a) elasto-plastic analysis and (b) strain softening analysis.

analysis, shear failure does occur at the crown and invert caused by high stress concentration. However, the failure zone does not extend so much interiorly into the rock, but is restricted within a thin region shaped like a cone. However, the tensile failure is at first initiated from the springline, and extends in an almost tangential direction to the tunnel surface.

For the case of strain softening analysis, although the general trend of the failure zone is virtually identical to that observed in the case of the elasto-plastic analysis, a great difference can be obviously recognized in the mode of failure at the crown and/or invert. Namely, the compressive failure is developed at the crown, almost similarly to the elasto-plasitic case. The stress in the failed element is relieved such that the state of stress results in the residual state and is transferred to adjacent elements. However, a most critical failure is then induced, as though surrounding the shear failure zone previously developed. We prefer to call the most critical failure in a numerical sense so that the element is identified to fail with the tensile failure as well as the shear failure occurring simultaneously. That is to say, the element fails completely and can not sustain any stress at all. The expansion of the shear failure zone is still further brought behind the zone of the most critical failure, and ceases to some extent as shown in Fig. 12.

The obtained results with regard to the mode of failure in the circumference of a tunnel would be very important to clarify a mechanism of tunnel instability, and would be reasonably consistent with the field observation. As in the case shown in Fig. 8 (b) when a tunnel is excavated in rock, in which a high horizontal stress remains, a significant instability is possibly caused at the crown. Lo and Morton[17] gave a brief description of roof instability based on a detailed inspection of a tunnel excavated in a shale formation in Ontario, Canada, where a considerably high horizontal stress (as high as 100kg/cm^2) remains in the rock[15]. The observation shows that the roof of the tunnel fell off due to the action of gravity, and the roof was then exposed in a "cone" shape as illustrated in Fig. 13 (a). The analytical result of Fig. 12 interprets remarkably well a phenomenon such as this.

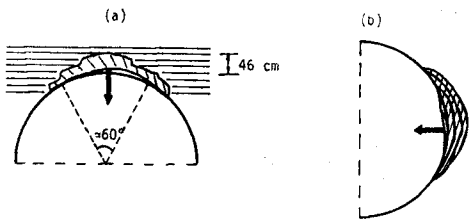

Fig. 13. Tunnel instability occasionally encountered: (a) falling off at the roof of tunnel excavated in a high horizontal stress field (after Lo and Morton[17]) and (b) rock burst at the side wall.

Meanwhile, when a tunnel is situated in such a situation as shown in Fig. 8 (c), a high overburden pressure would be then imposed on the tunnel in a vertical or subvertical direction. This situation can be readily obtained by rotating the coordinate axes in Fig. 12 at 90°. Correspondingly, in a case where the stress condition existing is sufficiently critical in excavating a tunnel, for example, a tunnel situated at a great depth, instability may then be caused at the side wall. In this phenomenon, a violent rupture may then be prone to arise, as occasionally encountered, in general, in a tunnel excavated in a mountain. Fig. 13 (b) illustrates schematically a rock burst at the side wall of a tunnel.

A detailed inspection of the rock falling at the roof and/or the rock burst at the side wall indicated that the ruptured rock pieces exhibited a slabbing and crushing, just as fractured by a tensile failure. The fractured zone is generally limited to a thin section in the surrounding rock, and extends within a region making a central angle of about 60°. These facts of observation suitably comfirm the results analytically obtained by taking into account the post-peak strain softening behavior of rock. Fig. 14 shows an appearance of a tensile crack developed in those element

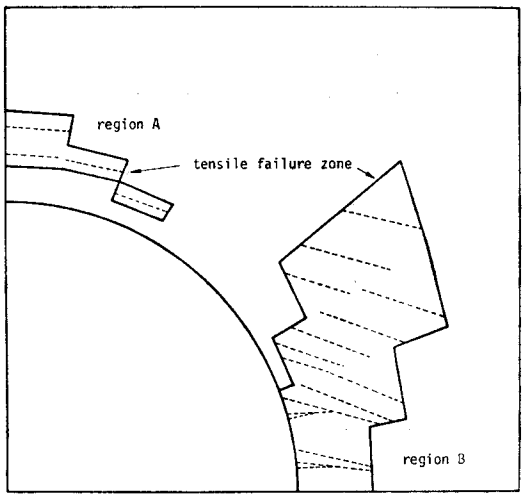

Fig. 14. Appearance of tensile cracks observed by the strain softeniing analysis.

which failed by the tensile failure. It may be noted from the figure that the crack developed in region A (where the most critical failure occurred) appears almost parallel to the surface of the tunnel, but almost perpendicular or obliquely to the surface in region B where the tensile failure solely occurred. An evident conclusion may then drawn that the appearance of the crack in region A significantly causes instability of the tunnel, such as the rock falling and/or the rock burst. On the

other hand, however, the crack in region B is conservative to the instability.

6. Conclusions

The mechanism of the instability of a tunnel, which has not satisfactorily been understood, was clarified in the present study by taking the intrinsic nature of rock like material, that is, the post-peak strain softening behavior, into consideration. The finite element method was successfully employed, with some modification, on the basis of the principle of the stress release and transfer method. Since little knowledge of the strain softening behavior of rock is available at this time, and since no versaitile constitutive law to be readily employed in the numerical analysis has yet been established, some ambiguous assumptions had to be made in the analysis. The obscurities concerning the strain softening behavior have to be manifested by further studies with regard to both experimental and theoretical viewpoints.

Nevertheless, the present fundamental study on the instability of a tunnel in consideration of the post-peak strain softening behavior of rock has led to an important finding. That is to say, when the stress condition in the circumference of a tunnel, induced by the excavation, is critical in relation to the failure strength of the rock, the "most critical failure" may then be caused in the region where the stress concentration arises. By the emergence of this failure, the rock in the zone completely loses resistance and therefore the stresses currently existing are entirely released in a moment. Since the tensile failure simultaneously incurs, accompanied with the shear faiure, a violent fracture is possibly caused in the rock. Such a phenomenon as this must therefore be closely related to the instability of the tunnel. The solution obtained by the analysis is fairly consistent with the field observations occasionally encountered, such as a falling off at the roof of a tunnel and rock burst.

Finally, it is emphasized that a precise knowledge concerning the rock properties as well as field data of in-situ stresses and geological discontinuities pre-existing rock formations, is a prerequisite for a rational design of underground cavities in rock and for the safety of any construction performance.

Acknowledgements

The present study was initiated when one of the authors, M. Hori, was working on the Faculty of Engineering Science, the University of Western Ontario, Ontario, Canada, under the general supervision of Professor K. Y. Lo, to whom the authors wish to acknowledge their gratitude for the valuable guidance of the field observations and the finite element program for the strain softening anaysis. Also, to Mr.

Clement Yuen, Ph. D. course student of the Geotechnical Section at the University of Western Ontario, the anthors are grateful for his valuable discussions during this present study. Since then, the numerical scheme has been refined and the investigation on the instability of tunnels has been clearly summarized. In preparing this paper, the authors wish to acknowledge their gratitude to Mr. Chikaosa Tanimoto, Research Associate in the Department of Civil Engineering, Kyoto University, for his valuable suggestions on the instability of tunnels, generally observed in the field.

References

1) G. C. Nayak and O. C. Zienkiewicz; Int. J. for Numerical Methods in Engineering, **5**, 113 (1972)
2) W. F. Brace; "State of Stress in the Earth's Crust", Elsevier, p. 110 (1964)
3) Z. T. Bieniawski, H. G. Denkhaus and U. K. Vogler; Int. J. Rock Mech. Min. Sci., **6**, 323 (1969)
4) D. C. Drucker; Proc. First UN Nat. Cong. Appl. Mech., p. 478 (1951)
5) Z. T. Bieniawski; Int. J. Rock Mech. Min. Sci., **4**, 395 (1967)
6) Z. T. Bieniawski; Rock Mechanics, **2**, 123 (1970)
7) T. Adachi and T. Ogawa; Preprint of the 32nd. Annual Meeting of JSCE, Part III, 341 (1977) (in Japanese)
8) B. Paul; J. Appl. Mech., **28**, 259 (1961)
9) J. C. Jaeger and N. G. W. Cook; "Fundamentals of Rock Mechanics", Methuen & Co. Ltd., p. 87 (1969)
10) O. C. Zienkiewicz, S. Valliappan and I. P. King; Geotechnique, **18**, 56 (1968)
11) K. Y. Lo and C. F. Lee; Proc. 8th. Int. Conf. Soil Mech. Found. Engng., Moscow, **1**, 251 (1973)
12) T. Kawamoto and T. Saito; Second Int. Conf. Numerical Methods in Geomechanics, Virginia Polytechnic Institute and State University, **1**, 791 (1976)
13) O. C. Zienkiewicz; "The Finite Element Method in Engineering Science" McGraw-Hill (1971)
14) M. Hori; under submitting to J. of JSCE (in Japanese)
15) J. H. L. Palmer and K. Y. Lo; Canad. Geotech. J., **13**, 1 (1976)
16) N. Hast; Phil. Tran. Roy. Soc. Lond., A, **274**, 409 (1973)
17) K. Y. Lo and J. D. Morton; Canad. Geotech. J., **13**, 216 (1976)